WILEY InterScience
DISCOVER SOMETHING GREAT

In vitro bioactivity and osteoblast response of porous NiTi synthesized by SHS using nanocrystalline Ni-Ti reaction agent

Y.W. Gu,[1,2] H. Li,[2] B.Y. Tay,[1] C.S. Lim,[3] M.S. Yong,[1] K.A. Khor[2]
[1]*Singapore Institute of Manufacturing Technology, 71 Nanyang Drive, Singapore 638075, Singapore*
[2]*School of Mechanical & Aerospace Engineering, Nanyang Technological University, Nanyang Avenue, Singapore 639798, Singapore*
[3]*School of Chemical & Biomedical Engineering, Nanyang Technological University, 16 Nanyang Drive, Singapore 637722, Singapore*

Received 2 November 2005; revised 9 December 2005; accepted 30 December 2005
Published online 24 April 2006 in Wiley InterScience (www.interscience.wiley.com). DOI: 10.1002/jbm.a.30743

Abstract: Porous NiTi with an average porosity of 55 vol % and a general pore size of 100–600 μm was synthesized by self-propagating high temperature synthesis (SHS) with the addition of mechanically alloyed nanocrystalline Ni-Ti as the reaction agent. The SHS of porous NiTi using elemental powders was also performed for comparison. To enhance the bioactivity of the metal surface, porous NiTi synthesized by nanocrystalline Ni-Ti was subjected to chemical treatment to form a layer of TiO_2 coating. The porous NiTi with TiO_2 coating was subsequently immersed in a simulated body fluid (SBF) to investigate its apatite forming ability. The effects of the addition of nanocrystalline Ni-Ti as reaction agent and the application of apatite coating on osteoblastic behavior were studied in primary cultures of human osteoblast cells. Results showed that the main phases in porous NiTi synthesized by elemental powders were NiTi, Ti_2Ni, and unreacted free Ni. By using nanocrystalline Ni-Ti as reaction agent, the secondary intermetallic phase of Ti_2Ni was significantly reduced and the free Ni was eliminated. TiO_2 coating with anatase phase was formed on the surface of porous NiTi after the chemical treatment. A layer consisting of nanocrystalline carbonate-containing apatite was formed on the surface of TiO_2 coating after soaking in SBF. The preliminary cell culture studies showed that the porous NiTi synthesized with the addition of nanocrystalline Ni-Ti attracted marked attachment and proliferation of the osteoblast cells. This gives the evidence of the potential biomedical applications of the porous NiTi. © 2006 Wiley Periodicals, Inc. J Biomed Mater Res 78A: 316–323, 2006

Key words: porous NiTi; SHS; apatite; nanocrystalline; cell culture

INTRODUCTION

NiTi alloy has been increasingly applied to medical and dental appliances and it is a promising implant material.[1–4] Attributed to its shape memory properties, it can be used to prepare functional implants activated at body temperatures.[5–7] The material also possesses high damping capacity and excellent superelastic properties.[8] However, views regarding the corrosion resistance and biocompatibility of NiTi in medical applications are conservative, mainly because of the high Ni content in the alloy, an element which is known to be toxic and allergenic.[9,10] TiO_2 coating on Ti alloy has been shown to enhance the corrosion resistance and biocompatibility.[11] The naturally formed oxide film is rather thin (a few tens of nanometer) and usually defective, passivation treatment of NiTi is necessary to thicken and improve the quality of TiO_2 oxide layer so as to improve the corrosion resistance and enhance the bioactivity.

It is an essential requirement that an apatite layer should be present on the material surfaces to act as the bonding interface between the materials and the living tissue, where the cells can preferentially proliferate and differentiate to produce apatite and collagen.[12,13] After that, the surrounding bone can then come into direct contact with the surface apatite and form tight chemical bonding. *In vitro* studies have demonstrated that the simulated body fluid (SBF) can be used to reproduce *in vivo* apatite layer formation on the surface of various materials after implantation.[14] Therefore, it is a most efficient method to immerse the porous NiTi samples with TiO_2 coating into SBF for the investigation of the biological behavior of porous NiTi and the biomimetic deposition of apatite layer.

Correspondence to: Y.W. Gu; e-mail: mywgu@ntu.edu.sg
Contract grant sponsor: Singapore Institute of Manufacturing Technology; contract grant number: U02-P-088B

So far, there is no report on the *in-vitro* apatite formation and osteoblastic behavior of porous NiTi produced by SHS with the addition of nanocrystalline Ni-Ti as the reaction agent. The addition of nanocrystalline powder to SHS NiTi effectively lowered the activation barriers for combustion synthesis reaction and therefore, it decreased the combustion temperature. Furthermore, the addition of nanocrystalline powder resulted in an improvement in the hardness and crack growth resistance in the SHS end-product.[15] In this study, chemical treatment was carried out at the temperature of 80°C to produce a TiO_2 layer. The chemically treated porous NiTi alloys were subsequently immersed in SBF for various periods of time to investigate their biomimetic apatite forming ability. The cell attachment in a primary culture of human osteoblast cells was investigated.

MATERIALS AND METHODS

Commercially elemental powders of titanium (~74 μm, 99.9% purity, CERAC, USA) and nickel (~5 μm, 99.9% purity, CERAC, USA) were used in this study. The elemental Ni-Ti powders with equiatomic composition were prepared by blending the powders using a tumbler mixer under argon atmosphere for 8 h at a speed of 65 rpm. The nanocrystalline Ni-Ti powders were prepared by mechanical alloying at 200 rpm for 75 h in the Retsch mill (Model PM-400) in argon atmosphere. The details for the preparation of nanocrystalline Ni-Ti can be found in our previous study.[16]

The powders were compacted into pellets with a diameter of 12.1 mm and the height of 20 mm by uniaxial die on WASBASH™ hydraulic press. The composition of the powders was 25 wt % nanocrystalline Ni-Ti + 75 wt % elemental Ni-Ti. The pellets with the composition of 100 wt % elemental Ni-Ti was also prepared for comparison. The green porosity of the two different types of samples was about 46 vol %,[17] which was calculated directly from the geometry and weight of the compacted samples. The ignition technique was employed for the synthesis of porous NiTi by using a plasma transferred arc (Thermal Arc Ultima 150). The induction furnace (Norax, Canada) was used to preheat the compacted powders at a temperature of 200°C.

The porous NiTi samples synthesized with the addition of nanocrystalline Ni-Ti as the reaction agent were cut into plates along the propagating direction, mechanically polished and ultrasonically cleaned before they were chemically treated with a solution containing 8.8*M* H_2O_2 and 0.1*M* HCl to form a layer of titania onto the surface of porous NiTi. The chemical treatment was performed at 80°C for 30 min. After chemical treatment, the samples were gently rinsed, dried in an oven at 60°C overnight, and heat treated at 400°C for 1 h. The samples were subsequently immersed in 50 mL of SBF solution in a continuously stirred bath containing distilled water with a stable temperature of 37°C for 7 days. The ionic concentration of the solution is 1.5 times higher than that of the human blood plasma (1.5 SBF). After immersion, the samples were removed from the solution, gently rinsed with distilled water, and dried at room temperature. The 1.5 SBF was prepared using Kokubo's formulation by dissolving reagent-grade mixtures of $CaCl_2$, $K_2HPO_4{\cdot}3H_2O$, KCl, NaCl, $MgCl_2{\cdot}H_2O$, $NaHCO_3$, and Na_2SO_4 in distilled water and buffering at pH 7.40 with tris-hydroxymethyl aminomethane and 1*N* hydrochloric acid (HCl) at 37°C.[18] The ion concentration of 1.5 SBF can be found in Ref. 19. The preliminary *in vitro* cell culture work was conducted for the samples using the hFOB 1.19 cell line. This cell line was established by transfection of limb tissue obtained from a spontaneous miscarriage. The autoclaved Ni-Ti samples were incubated in 12-well plate using the culture medium (Dulbecco's modified eagle medium (DMEM) containing 10% fetal bovine serum (FBS) and 0.5% antibiotics). The cells were cultured in an atmosphere of 100% humidity, 5% CO_2, and 37°C in 12-well culture plates (with 1mL media contained in each well). After 2 days

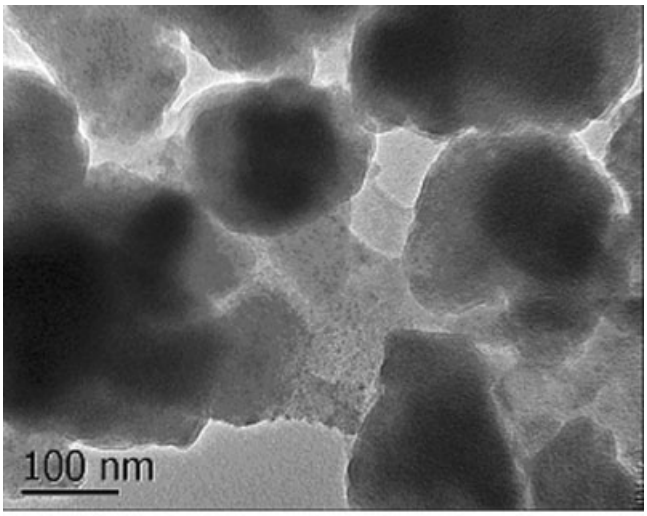

(a)

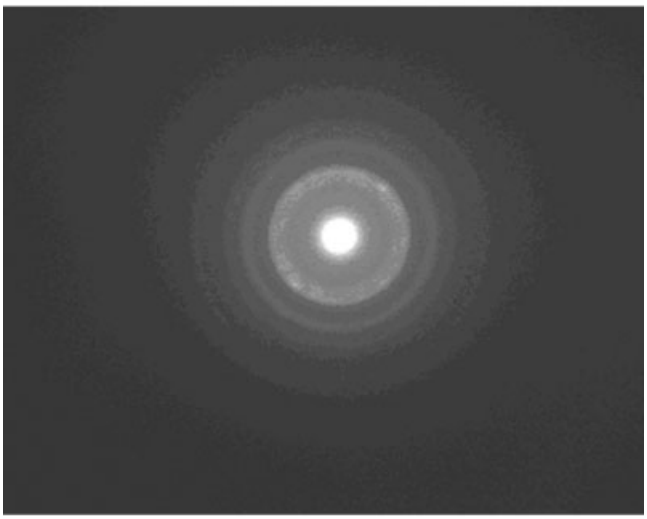

(b)

Figure 1. TEM bright field image of nanocrystalline Ni-Ti powders and the correspondence electron diffraction pattern. a: Bright field image. b: Electron diffraction pattern.

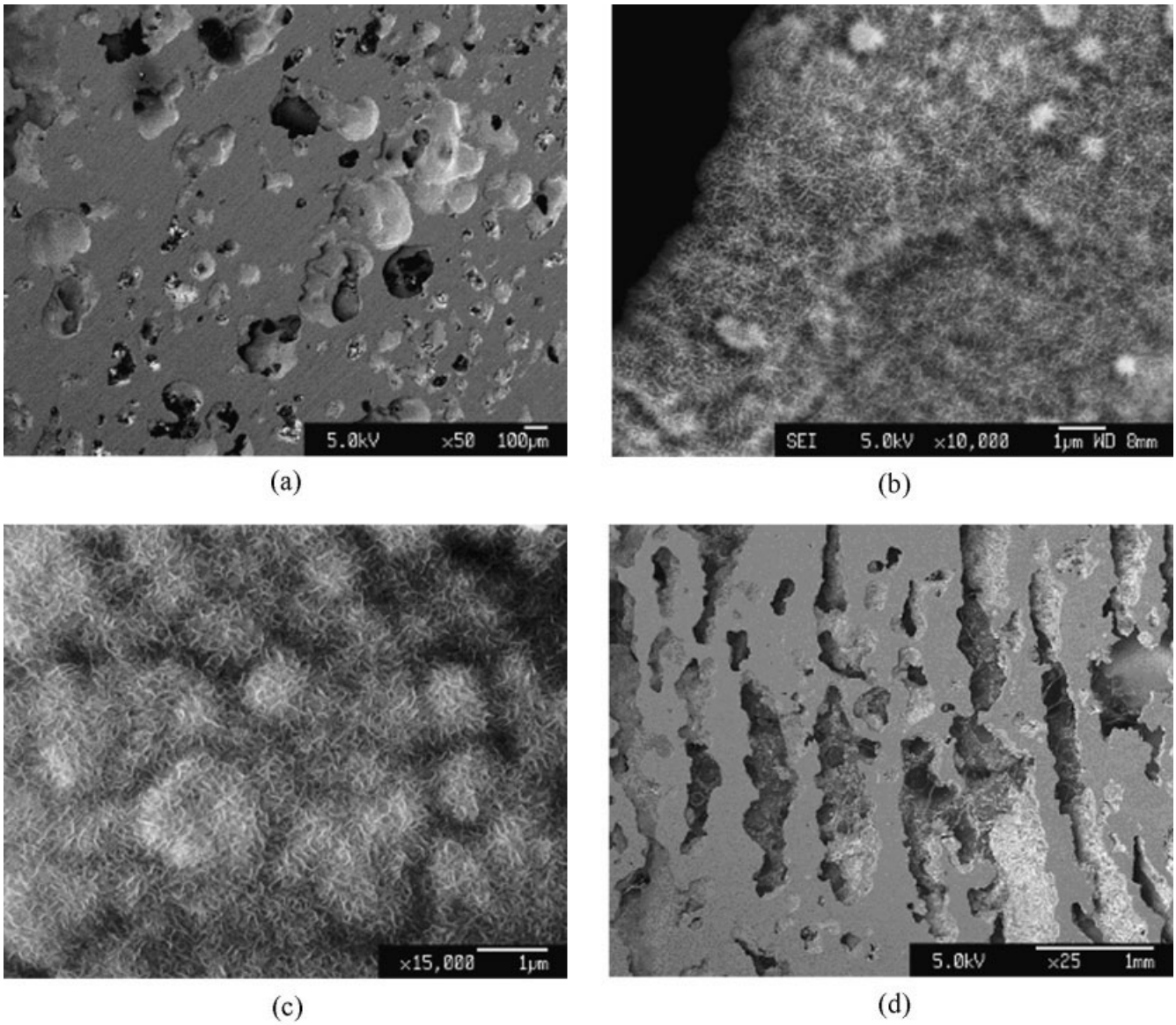

Figure 2. Surface morphology of porous NiTi. a: Untreated porous NiTi synthesized with the addition of nanocrystalline Ni-Ti as reaction agent. b: After chemical treatment. c: After immersion in 1.5 SBF for 7 days. d: Untreated porous NiTi synthesized by elemental powders.

incubation, the morphology of the cells attached onto the samples was observed by a JEOL JSM-6340F field emission scanning electron microscopy (FE-SEM). Prior to the SEM observation, 2.5% glutaraldehyde in 0.1*M* sodium cacodylate buffer was used for prefixing the cells, followed by postfixation with 1% osmium tetroxidein in 0.1*M* cacodylate buffer. The final steps for fixing the samples were dehydration and critical point drying.

The morphology and crystallite size of the nanocrystalline Ni-Ti powders were examined by a JEOL 2000 transmission electron microscopy (TEM) operated at 200 kV. The morphologies of the surface of the porous NiTi samples were examined by FE-SEM equipped with an energy dispersive spectroscopy (EDX) unit. The general porosity of SHS porous NiTi was performed on image analyzer (Cambridge Instruments Leica™ Quantimet 570). The thin film X-ray diffraction (TF-XRD) measurement was performed on a Philips X'pert X-ray diffractomer (Cu Kα radiation, 40 kV, 30 mA, grazing incidence at 5°). The elemental composition and surface chemistry of the samples were determined by X-ray photoelectron spectroscopy (XPS). XPS spectra were recorded on a Kratos spectrometer operated using Al $K_{\alpha 1,2}$ (1486.6 eV) excitation. The survey spectra in the range of 0–1100 eV was recorded in 1 eV step for each sample followed by high resolution spectra over different element peaks in 0.1 eV steps. The atomic concentrations were calculated from the measured peak areas using sensitivity factors. Curve fitting was performed after a Shirley background subtraction by a nonlinear least square fit. The pressure of the analysis chamber was lower than 10^{-7} Pa, which was increased to $\sim 5 \times 10^{-5}$ Pa during ion bombardment. For elemental depth profiling, an ion gun (Kratos MacroBeam) of 4 keV energy was used with high purity Ar gas. The etching rate is about 2.5 nm/min and the etching time is

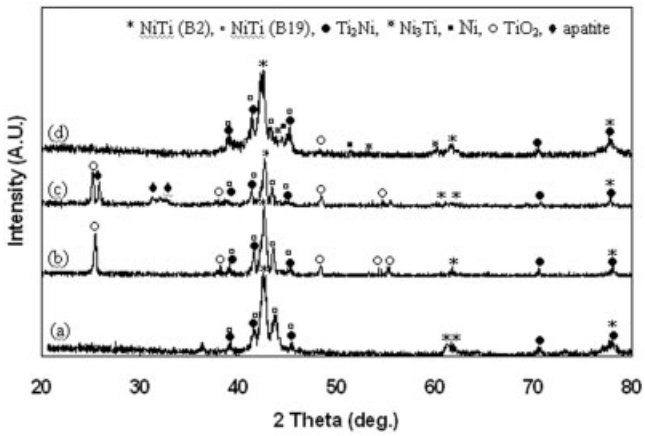

Figure 3. XRD patterns of the porous NiTi. a: Untreated porous NiTi synthesized with the addition of nanocrystalline Ni-Ti. b: After chemical treatment. c: After immersion in 1.5 SBF for 7 days. d: Untreated porous NiTi synthesized by elemental powders.

400 s. Calibration is done by using the binding energy of C 1s line at 284.6 eV.

RESULTS AND DISCUSSION

Figure 1 shows the TEM bright field image of the nanocrystalline Ni-Ti powder. The particles with sizes of around 10–150 nm can be observed. The corresponding electron diffraction pattern contains lattice diffraction rings, which suggests the formation of nanocrystalline Ni-Ti alloy.

The surface morphology of untreated porous NiTi synthesized with the addition of nanocrystalline Ni-Ti as reaction agent is shown in Figure 2(a). The morphologies of the samples after chemical treatment and after immersion in 1.5 SBF for 7 days are shown in Figure 2(b,c), respectively. The porous NiTi has a pore size of 100–600 μm with general porosity of 55 vol %. It was found that the most of the pores exist three-dimensionally as interconnected pore structures by examining in the cross-sectional direction.[17] The pore shape is near circular or elliptic, as shown in Figure 2(a). The pore size between 100 and 600 μm with a general porosity of 55 vol % is favorable for osseointegration for biomedical application. After chemical treatment in H_2O_2/HCl solution at 80°C for 30 min, the surface of porous NiTi is completely covered by a layer of crystals, as shown in Figure 2(b). This layer

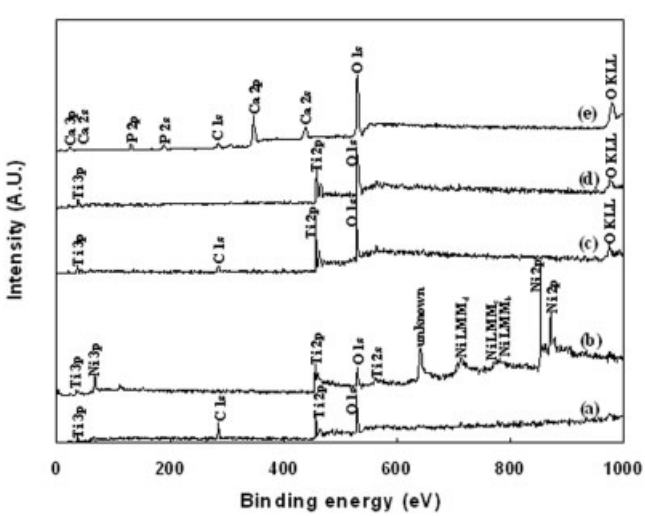

Figure 4. XPS survey spectra of porous NiTi. a: Untreated porous NiTi synthesized with the addition of nanocrystalline Ni-Ti as reaction agent, before etching. b: Sample (a), after etching. c: Sample after chemical treatment, before etching. d: Sample (c), after etching. e: Sample after immersion in 1.5 SBF for 7 days.

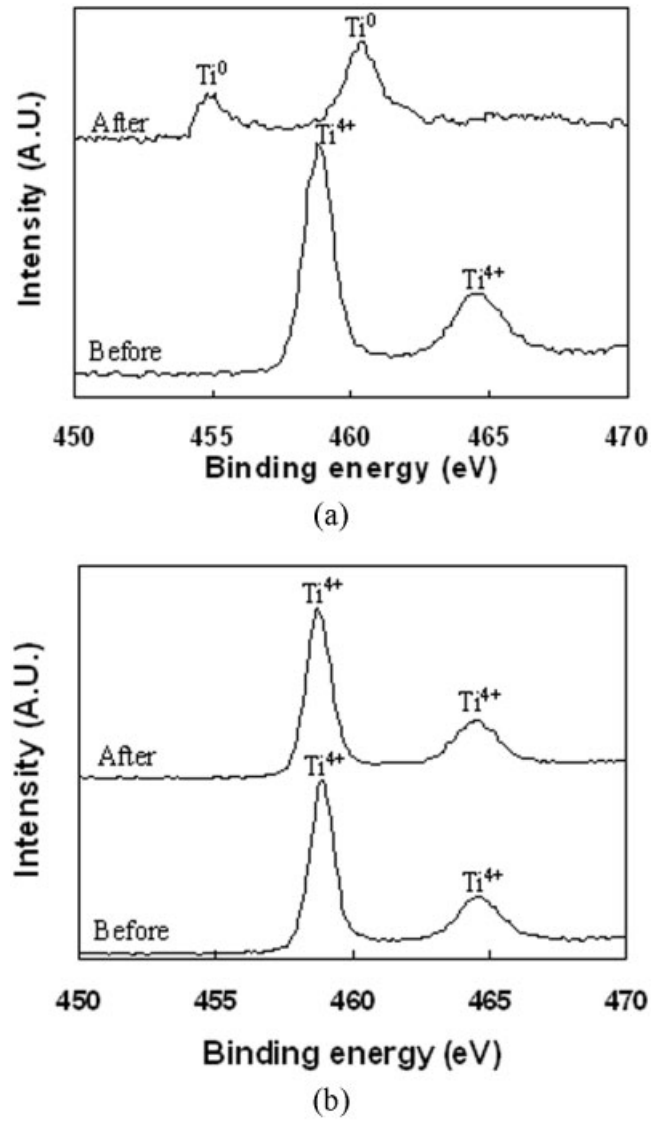

Figure 5. High resolution Ti 2p spectra before and after etching. a: Untreated porous NiTi synthesized with the addition of nanocrystalline Ni-Ti as reaction agent. b: after chemical treatment.

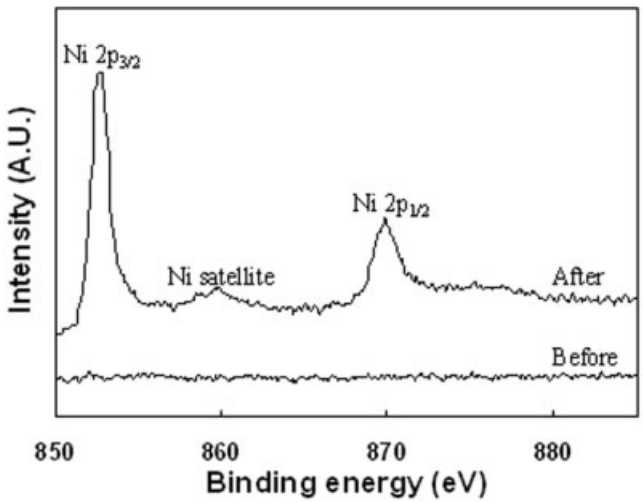

Figure 6. High resolution Ni 2p spectra before and after etching.

appears to be consisting of many nanosized spheroidal crystallites and nanosized pores. The thickness of the layer is about 0.7 μm as determined by cross-sectional SEM. EDX analysis reveals that this layer is rich in Ti and O. The chemically treated porous NiTi was subsequently immersed in 1.5 SBF for 7 days to study its bioactivity. As can be observed from Figure 2(c), a flake-like layer is formed on the surface of the sample and the crystals are composed of many nanosized crystallites. The thickness of the layer is about 1.8 μm. EDX analysis reveals that this layer is Ca and P rich phase. For comparison purpose, the surface morphology of the porous NiTi synthesized by pure elemental powders is shown in Figure 2(d). The pores exist perpendicularly to the propagation direction and the cavities appear in the arrays of circular conduits, with many near circular or elliptical small pores distributed uniformly in the banded structure of channels. The porous NiTi synthesized by elemental powders has an average width of channels ranging from 1 to 3.5 mm with a general porosity of 45 vol %.[16] The differences in the pore shape of the porous NiTi synthesized by the powders with and without the addition of nanocrystalline Ni-Ti could be due to the differences in the particle size and the energy stored in the powder. The mechanically alloyed nanocrystalline Ni-Ti has much smaller particle size compared to the elemental powders, and greater energy stored in the powders through atomic arrangement in the cores of defect such as grain boundaries, interphase boundaries, or dislocations resulted from the mechanical alloying process. The highly exothermic reaction and the small crystallite size of the nanocrystalline Ni-Ti lead to a greater fraction of molten liquid and bring forth greater capillary forces to attract the particles together.[20] Therefore, most of the linear elongated channels as observed in the elemental porous NiTi transform into smaller pores in the porous NiTi with the addition of nanocrystalline NiTi.

Figure 3 shows the XRD patterns of the untreated porous NiTi synthesized with the addition of nanocrystalline Ni-Ti, and that subjected to chemical treatment in H_2O_2/HCl solution, and followed by immersion in 1.5 SBF. The XRD pattern of porous NiTi synthesized by elemental powders is also shown in Figure 3 for comparison. As can be observed from Figure 3, apart from the main phases of NiTi(B2) and NiTi(B19) in the porous NiTi synthesized by the pure elemental powders, the secondary phases such as Ti_2Ni and the unreacted free Ni are also found. It is well documented that Ni is considered to be responsible for the clinical toxic and allergic responses, and thus, it often causes suspicion of its suitability for medical use.[21] With the addition of nanocrystalline Ni-Ti as the reaction agent, the free Ni peak disappears. Quantitative XRD analysis reveals that there is

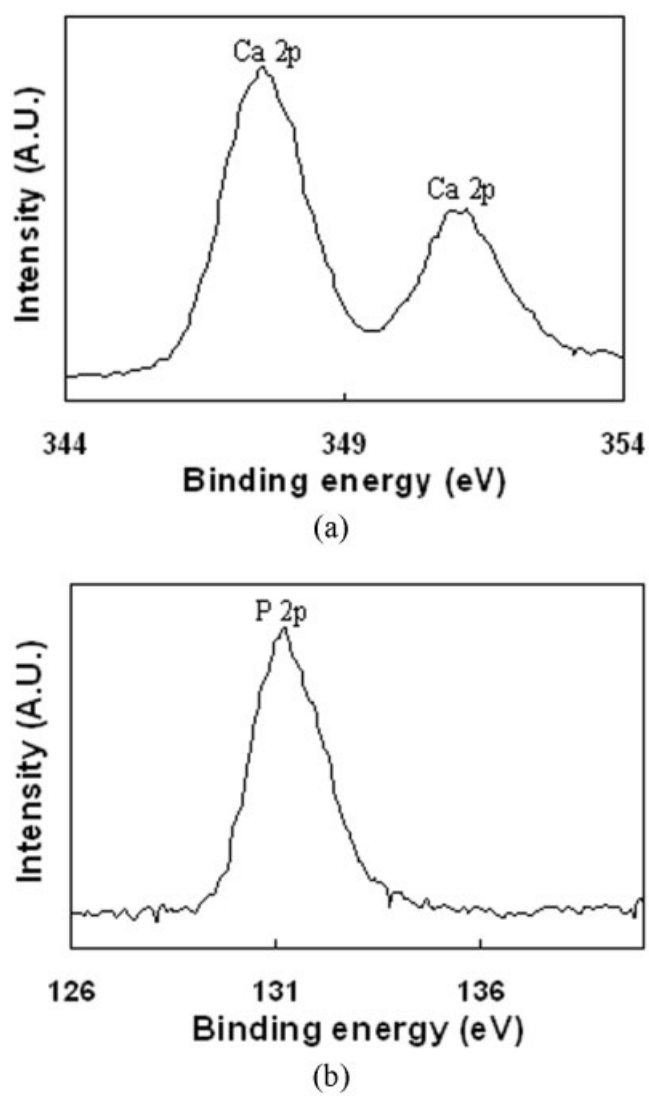

Figure 7. High resolution Ca 2p and P 2p spectra. (a) Ca 2p and (b) P 2p.

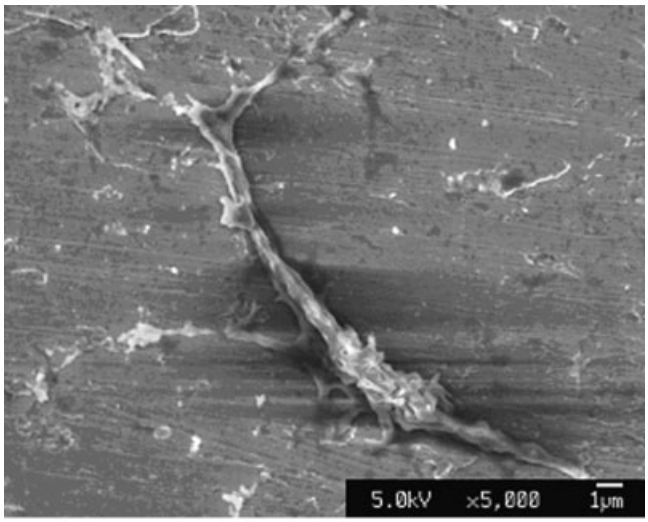

(a)

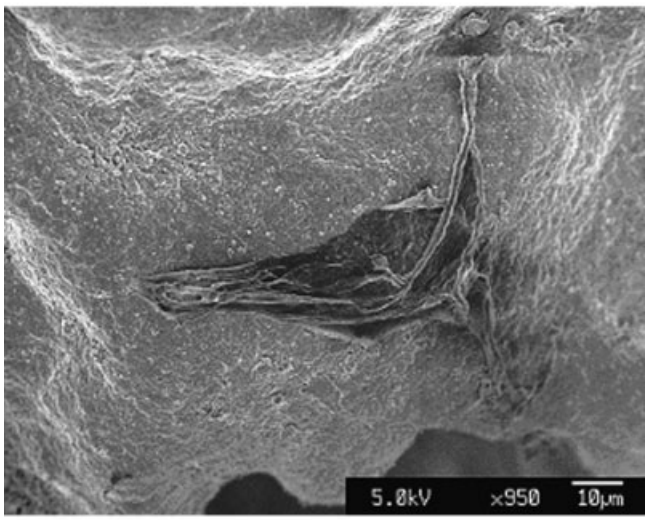

(b)

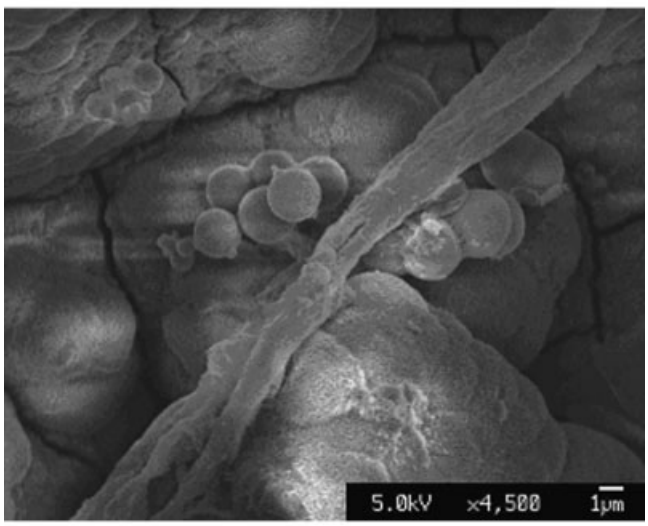

(c)

Figure 8. Typical FESEM pictures showing the osteoblast cells attached on the sample surfaces after 2 days culturing. a: Untreated porous NiTi synthesized with the addition of nanocrytalline Ni-Ti. b: Porous NiTi with TiO_2 coating. c: Porous NiTi with TiO_2/apatite duplex coatings.

a significant reduction in the amount of Ti_2Ni, with an increase in the amount of NiTi phase. This is probably due to the smaller particle size and the greater energy stored in the nanocrystalline powders, which effectively lowers the activation barriers for combustion synthesis reaction and aids the sintering process. The XRD result of chemically treated porous NiTi synthesized with the addition of nanocrystalline Ni-Ti indicates the presence of anatase, which reveals that the layer of crystals as shown in Figure 2(b) is TiO_2. The XRD pattern of the surface of porous NiTi subjected to chemical treatment followed by immersion in 1.5 SBF shows the presence of apatite peaks at 2θ of 26–32. It is therefore confirmed that the flake-like structure, covering the surface of porous NiTi after immersion in 1.5 SBF, is apatite.

The surface species present on the surfaces and the elemental composition were studied using XPS. Figure 4 shows the XPS survey spectra of the surfaces of untreated porous NiTi, TiO_2 layer, and apatite layer. The high resolution Ti 2p and Ni 2p spectra before and after etching are shown in Figures 5 and 6, respectively. There is no significant difference in the survey spectra of the untreated and chemically treated porous NiTi before etching. The elements present on their surfaces are Ti and O. After etching, there is almost no change in the spectra for the chemically treated porous NiTi. However, significant change can be observed for the untreated porous NiTi. Besides the presence of Ti, peaks corresponding to Ni are also observed. This implies that the surface of untreated porous NiTi is covered by a thin layer of oxide. High resolution Ti 2p before etching shows a doublet consisting of Ti $2p_{1/2}$ and Ti $2p_{3/2}$: two strong Ti^{4+} peaks, that is, $2p_{1/2}$ (Ti^{4+}, 464.6 eV) and $2p_{3/2}$ oxide (Ti^{4+}, 458.8 eV). After etching, the surface of chemically treated sample still shows the presence of two Ti^{4+} peak. However, it can clearly be observed that Ti is mostly present as Ti^0 (Ti-Ti) for the untreated porous NiTi sample after etching. The presence of Ti^{2+} (TiO) and Ti^{3+} (Ti_2O_3) can also be observed. This is in consistence with the previous study on the depth analysis of Ti 2p for heat treated NiTi,[22] which showed that Ti^{4+} decreases and the metallic Ti increases significantly with increasing depth. In addition, both TiO (Ti^{2+}) and Ti_2O_3 (Ti^{3+}) first increased and then gradually decreased with increasing depth.[20] In other words, TiO_2 is partly reduced to lower oxides with depth. This indicates that the titanium oxide on the surface of untreated porous NiTi is present as a mixture of oxide states and the

titanium oxide layer is rather thin. As for the chemically treated porous NiTi, no Ti^0, Ti^{2+}, and Ti^{3+} are detected on the surface after etching, indicating a thicker layer of TiO_2. For the Ni 2p spectra before and after etching as shown in Figure 6, no Ni peak can be observed for the sample before etching, which implies that the surface of NiTi is covered by a thin layer of titanium oxide. After etching, the XPS spectrum shows the presence of Ni peaks, with two distinct metallic peaks of Ni $2p_{3/2}$ at 852.6 eV and Ni $2p_{1/2}$ at 869.7 eV.

After immersion in 1.5 SBF for 7 days, the peaks corresponding to Ti 2p are disappeared from the spectrum, while Ca 2p, Ca 2s, Ca 3p, P 2s, P 2p, O 1s, and C 1s are identified, as shown in Figure 4. The disappearance of Ti 2p peak indicates the formation of CaP layer on the surface of porous NiTi. The high resolution Ca 2p and P 2p spectra shown in Figure 7 reveal that the Ca 2p spectrum is a doublet with Ca $2p_{3/2}$ and Ca $2p_{1/2}$ at 347.4 and 351.0 eV, respectively. P 2p peak is symmetric and has a binding energy of 133.1 eV, which reveals its stable binding energy in apatite. This indicates that the precipitant on porous NiTi is apatite.[23] Quantitative elemental analysis of Ca:P ratio of the apatite layer is 1.33, which is much lower than those of stoichiometric hydroxyapatite (HA) (1.67) and amorphous calcium phosphate (ACP) (1.50). The apatite formed on the surface of NiTi alloy has structure and chemical composition similar to that of natural bone.

After the 2 days incubation in the cell culture medium, the porous NiTi synthesized by elemental powders shows no cell attachment. This is due to the presence of unreacted free Ni, as Ni is toxic and allergenic. However, the treated samples, that is, the porous NiTi synthesized with the addition of the nanocrystalline Ni-Ti, the porous NiTi with TiO_2 coating, and the porous NiTi with apatite coating, showed very well attached and proliferated cells on their surfaces (Fig. 8). The well stretched structure of the cells (Fig. 8) indicates fast proliferation and differentiation of the cells. It therefore proves that the treatment via nanocrystalline Ni-Ti addition, TiO_2 coating, or apatite coating can effectively make the NiTi samples bioactive. To elucidate the proliferation rates of the cells on the sample surfaces and clarify the difference in bioactivity of the treated NiTi samples, further work is being conducted.

CONCLUSIONS

The porous NiTi with an average porosity of 55 vol % and a general pore size of 100–600 μm was synthesized by SHS using nanocrystalline Ni-Ti as the reaction agent. With the addition of nanocrystalline Ni-Ti as the reaction agent, the secondary intermetallic phase of Ti_2Ni was diminished and the unreacted free Ni was eliminated in the porous NiTi compared to the NiTi synthesized by the pure elemental powders. A layer of nanocrystalline TiO_2 coating was deposited on the surface of porous NiTi by chemical treatment in H_2O_2/HCl solution. The TiO_2 coating was found to possess good bioactivity when immersed in the SBF solution for the apatite formation. The apatite layer formed *in vitro* had a Ca:P ratio of 1.33, which is similar to that of the human bone. Culturing of the osteoblast cells on the samples showed that the treatment, that is, addition of nanocrystalline Ni-Ti reaction agent, formation of TiO_2 layer, or being coated with apatite, for the porous NiTi is effective in improving the bioactivity of the samples. The promising biocompatibility of the samples has been evidenced by the well attachment and proliferation of the cells.

The authors are grateful to Mr. C.W. Goh for the preparation of SHS NiTi samples.

References

1. Kapanen A, Ilvesaro J, Danilov A, Ryhanen J, Lehenkari P, Tuukkanen J. Behavior of nitinol in osteoblast-like ROS-17 cell cultures. Biomaterials 2002;23:645–650.
2. Hernandez R, Polizu S, Turenne S, Yahia L. Characteristics of porous nickel-titanium alloys for medical applications. Biomed Mater Eng 2002;12:37–45.
3. Dai K. Studies and applications of NiTi shape memory alloys in the medical field in China. Biomed Mater Eng 1996;6:233–240.
4. Fu YQ, Du HJ, Huang WM, Zhang S, Hu M. TiNi-based thin films in MEMS applications: A review. Sens Actuators 2004;112: 395–408.
5. Kujala S, Ryhanen J, Jamsa T, Danilov A, Saaranen J, Pramila A, Tuukkanen J. Bone modeling controlled by a nickel-titanium shape memory alloy intramedullary nail. Biomaterials 2002;23: 2535–2543.
6. Li BY, Rong LJ, Li YY, Gjunter VE. Electric resistance phenomena in porous Ni-Ti shape-memory alloys produced by SHS. Scripta Mater 2001;44:823–827.
7. Filip P, Musialek J, Lorethova H, Nieslanik J, Mazanec K. TiNi shape memory clamps with optimized structure parameters. J Mater Sci: Mater Med 1996;7:657–663.
8. Itin V, Gyunter VE, Shabalovskaya SA, Sachdeva RLC. Mechanical properties and shape memory of porous nitinol. Mater Character 1994;32:179–187.
9. Chen MF, Yang XJ, Liu Y, Zhu SL, Cui ZD, Man HC. Study on the formation of an apatite layer on NiTi shape memory alloy using a chemical treatment method. Surf Coat Technol 2003;173: 229–234.
10. Rondelli G, Vicentini B. Bone modeling and cell–material interface responses induced by nickel–titanium shape memory alloy after periosteal implantation. Biomaterials 1999;20:1309–1317.
11. Cheng FT, Shi P, Man HC. A preliminary study of TiO_2 deposition on NiTi by a hydrothermal method. Surf Coat Technol 2004;187:26–32.
12. Hench LL. Bioceramics. J Am Ceram Soc 1998;81:1705–1728.
13. Kokubo T, Kushitani H, Kitsugi S, Yamamuro T. Solutions able to reproduce in vivo surface structure changes in bioactive glass-ceramic A-W. J Biomed Mater Res 1990;24:721–734.

14. Kokubo T, Ito S, Huang ZT, Hayashi T, Sakka S, Kitsugi T, Yamamuro T. Ca,P-rich layer formed on high-strength bioactive glass-ceramic A-W. J Biomed Mater Res 1990;24:331–343.
15. Goh CW, Gu YW, Lim CS, Jarfors AEW, Tay BY, Yong MS. Effect of using mechanically alloyed reaction agent on self-propagating high temperature synthesis of porous NiTi. In: Khor KA, Ramanujan RV, Ooi CP, Zhao JH, editors. Proceedings of 3rd International Conference on Materials Processing for Properties and Performance. Institute of Materials East Asia; 2004. p 905–912.
16. Gu YW, Goh CW, Goi LS, Lim CS, Jarfors AEW, Tay BY, Yong MS. Solid state synthesis of nanocrystalline and/or amorphous 50Ni-50Ti alloy. Mater Sci Eng A 2005;392:222–228.
17. Goh CW, Gu YW, Lim CS, Tay BY. Influence of nanocrystalline Ni-Ti reaction agent on self-propagating high-temperature synthesized porous NiTi. Intermetallics. Forthcoming.
18. Kokubo T. Bonding mechanism of bioactive glass-ceramic A-W to living bone. In: Yamamuro T, Hench LL, Wilson J, editors. CRC Handbook of Bioactive Ceramics, Vol I. Boca Raton, FL: CRC Press; 1990. p 41–49.
19. Gu YW, Tay BY, Lim CS, Yong MS. Biomimetic deposition of apatite coating on surface-modified NiTi alloy. Biomaterials 2005;26:6916–6923.
20. Moore JJ, Feng HJ. Combustion synthesis of advanced materials. I. Reaction parameters. Prog Mater Sci 1995;39:243–273.
21. Humbeeck J, Stalmans R, Besselink PA. Shape memory alloys. In: Helsen JA, Breme HJ, editors. Metals as Biomaterials. Chichester: Wiley; 1998. p 73–100.
22. Gu YW, Tay BY, Lim CS, Yong MS. Characterization of bioactive surface oxidation layer on NiTi alloy. Appl Surf Sci 2005;252: 2038–2049.
23. Feng B, Chen JY, Qi SK, He L, Zhao JZ, Zhang XD. Characterization of surface oxide films on titanium and bioactivity. J Mater Sci: Mat Med 2002;13:457–464.